SELF-IGNITION OF HYDROGEN-NITROGEN MIXTURES DURING HIGH-PRESSURE RELEASE INTO AIR

Rudy, W.[1], Teodorczyk, A.[2] and Wen, J.[3]
[1] Warsaw University of Technology, Institute of Heat Engineering, Nowowiejska 21/25, 00-665, Warsaw, Poland, wrudy@itc.pw.edu.pl
[2] Warsaw University of Technology, Institute of Heat Engineering, Nowowiejska 21/25, 00-665, Warsaw, Poland, ateod @itc.pw.edu.pl
[3] University of Warwick, School of Engineering, Coventry C4 7AL, England, jennifer.wen@warwick.ac.uk

ABSTRACT

This paper demonstrates experimental and numerical study on spontaneous ignition of H_2-N_2 mixtures during high-pressure release into the air through the tubes of various diameters and lengths. The mixtures included 5% and 10% (vol.) N_2 addition to hydrogen being at initial pressure in range of 4.3 - 15.9 MPa. As a point of reference pure hydrogen release experiments were performed with use of the same experimental stand and extension tubes. The results showed that N_2 addition may increase the initial pressure necessary to self-ignite the mixture as much as 2.08 or 2.85 - times for 5% and 10% N_2 addition respectively. Additionally, simulations were performed with use of Cantera code (0-D) based on the ideal shock tube assumption and with the modified KIVA3V code (2-D) to establish the main factors responsible for ignition and sustained combustion during the release.

1.0 INTRODUCTION

Hydrogen as a fuel seems to be environmentally "clean" as the main combustion product in air is water vapour. Hydrogen has a very high (120 MJ/kg) lower heating value (LHV) per mass unit, wide flammability range (4 – 75 % vol. in air) and low ignition energy (0.02 mJ), which promotes hydrogen in many combustion applications. Unfortunately due to the hydrogen's low density, volume based LHV is very low. This feature demands liquefaction or pressurization of hydrogen to fulfil reasonable fuel tank dimensions requirement. Liquefied hydrogen demands low temperature storage (~ 20 K) and highly heat insulating tanks with necessary controlling systems (significant cost and mass). Additional energy looses are due to the liquefaction process and ortho– to para–hydrogen conversion [1]. As regards gaseous hydrogen, commercially available high-pressure tanks have working pressures of 35 - 70 MPa, prototypes even with 105 MPa. Nevertheless hydrogen energy volumetric density in the tank is still highly below the standard gasoline or diesel oil energy densities. However, due to the well known, relatively simple and cheap technology high–pressure is still the most widespread method for hydrogen storage. High-pressure tanks create risk of hydrogen uncontrolled release (caused by e.g. tank burst, puncture, control system failure, tank overheat, material defects, etc.), dispersion and in the presence of the ignition source the following deflagration occurs with possible deflagration to detonation transition (DDT).

High pressure hydrogen ignition during discharge into the air and without a distinct ignition source had been reported for the first time in the 20s of the 20th century [2]. In the 70s of the 20th century 'diffusion ignition' was described as an ignition in a thin diffusion layer between hydrogen and pre-heated air by leading shock wave [3]. In recent years one could observe an increased interest in hydrogen technologies and safety issues corresponding to them, including uncontrolled ignition during discharge into the air from high-pressure installations. Latest experimental [4-18] as well numerical [19-24] works focus mainly on the detailed description of the self-ignition mechanism according to different initial and boundary conditions including: extension channel geometry: diameter [4-7,19], length [5-17,20-22], cross-section shape [8-7,18,23] or obstacle presence in front of the hydrogen stream [18,24]. Despite of this research there is still lack of experimental data concerning the influence of different gases doping to hydrogen on the self-ignition occurrence. This kind of data would allow to

understand the nature of the self-ignition phenomenon itself and deliver the knowledge necessary for prevention or promotion (if desirable) self-ignition process.

2.0 EXPERIMENTAL RESEARCH

2.1 Experimental stand and procedure

The experimental stand used was previously utilized for hydrogen and hydrogen-methane mixtures self-ignition process [25]. The experimental stand was divided into three main sections (see Fig. 1):

- air section – rectangular tube 0.11x0.11x1 m,
- data acquisition system (DAS), PCB type 113B24 and 113B22 pressure gauges, photodiodes, ion probes, computer, amplifier, time unit,
- high-pressure section (gas cylinders, single acting air-driven booster Haskel AG-75, high-pressure line, pressure accumulator, electromagnetic valve (EMV).

High pressure release was created with the use of diaphragm which separated air section and high-pressure section and ruptured at different initial pressures depending on the diaphragm material and thickness. The diaphragm was made of metal sheet of aluminium, copper or brass. The majority of the experiments were conducted with the use of aluminium diaphragm with thicknesses: 0.1, 0.15, 0.2, 0.25 mm.

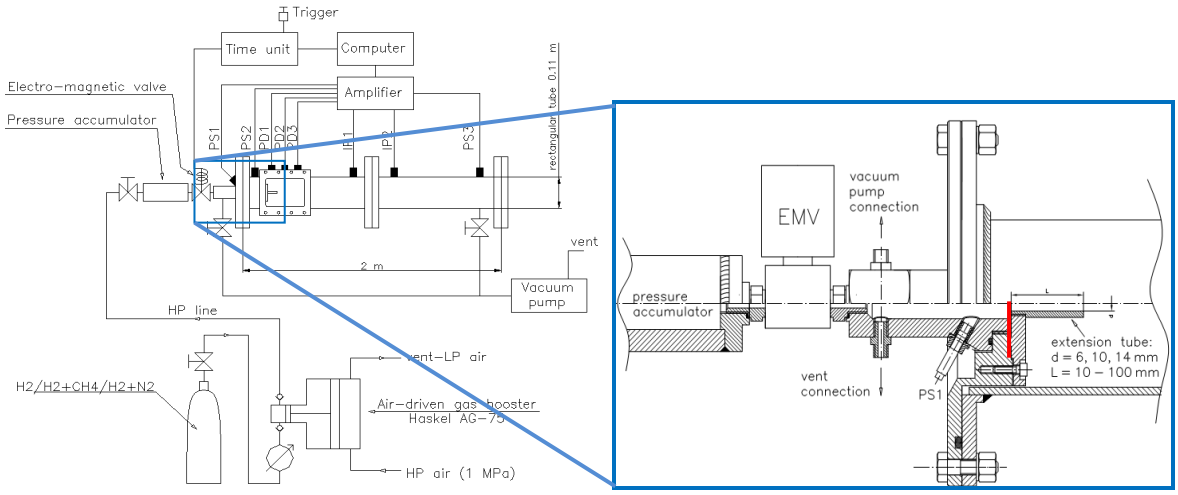

Figure 1. Experimental stand scheme (left) and detailed cross section (right) of the diaphragm holder with extension tube. Diaphragm marked in red.

The sensors positions with regards to the diaphragm and flow direction were as follows (PS – pressure sensors, IP – ion probes, PD – photodiodes):

- PS1 – 30 mm upstream,
- PS2 – 60 mm downstream,
- PS3 – 860 mm downstream,
- IP1 – 360 mm downstream,
- IP2 – 560 mm downstream,
- PD1 – 100 mm downstream,
- PD2 – 125 mm downstream,
- PD3 – 150 mm downstream.

Each experiment started with hydrogen or hydrogen-nitrogen mixtures compression to a design pressure which exceeded by around 1 MPa the approximated diaphragm burst-pressure. The gas was compressed in a pressure accumulator. The gas in the volume between diaphragm and EMV was evacuated with the use of vacuum pump. The DAS recording was activated 5 µs after EMV activation which lasted for 30 ms. The gas depressurised through the EMV into the evacuated volume. The diaphragm burst when pressure forces reached diaphragm ultimate strength and the high-pressure gas

depressurized into the air through the extension tube. After each single experiment the gas in the air section was evacuated, filled with ambient air and disassembled in order to fit a new diaphragm, reassembled and the procedure started from the beginning.

2.2 Results

In total, 295 experiments were conducted for hydrogen-nitrogen mixtures release: 213 for 5% N_2 and 82 for 10% N_2 addition. The results obtained for pure hydrogen release reported in previous work [25] (344 experiments) and slightly updated [26] (360 experiments) were treated as a point of reference. Typical recordings of the sensors for cases with and without ignition are presented in Fig. 2. The cases with and without ignition may be clearly distinguished. The sound effects accompanying the experiments with ignition were also higher than in case of non-ignition cases. In case of ignition, shortly after the diaphragm ruptures (abrupt decrease in PS1 indication) and gas leaves the extension tube, photodiodes give clear signal, simultaneously sensor PS2 gives a signal of shock wave which is attenuated by the fact that PS2 sensor is placed at the bottom of the tube and upstream of the flow with reference to the extension tube exit. Next sensor which gives a signal is PS3 sensor placed 80 mm from the end of the tube. Ion probes show that the ignited jet flame is sustained and affected by the shock wave as further oscillations have been recorded. Oscillations in PS2 and PS3 sensors indicate reflection form the tube ends. In general, the above scheme of the single experiment with ignition was similar for pure hydrogen and hydrogen-nitrogen mixtures releases.

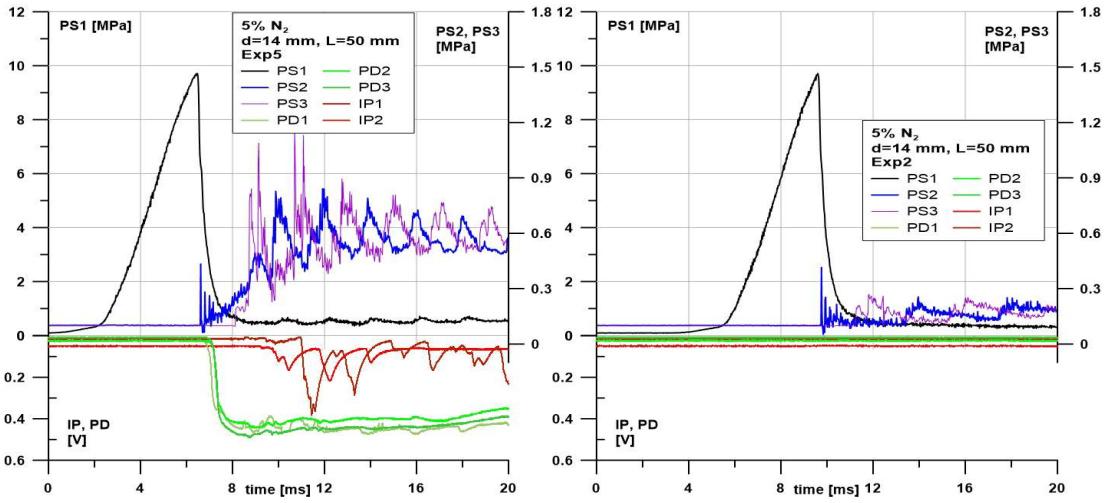

Figure 2. Sensors indications for cases with (left, P_{burst} = 9.76 MPa) and without ignition (right, P_{burst} = 9.77 MPa); d = 14 mm, L = 50 mm.

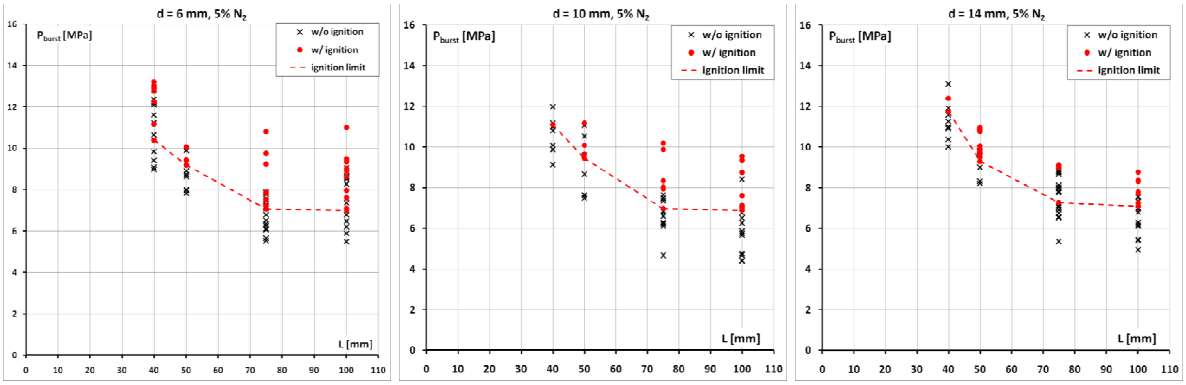

Figure 3. Cumulative diagrams of burst pressure ignition limit obtained for various extension channel lengths (40-100 mm) and diameters (6, 10, 14 mm) for cases with 5% N_2 addition to hydrogen.

The ignition if occurred was recorded by both photodiodes and ion probes therefore there were no single experiment with 'failed ignition' – quenched ignition shortly after leaving the tube as it was observed with hydrogen-methane mixture [26] or for pure hydrogen release reported in the literature [4,10,11,14].

Figures 3 and 4 show the cumulative diagrams burst pressure-tube length dependence for 5% and 10% N_2, respectively. Figure 5 shows the comparison between ignition limit curves obtained for pure hydrogen and hydrogen-nitrogen mixtures. Experiments showed that hydrogen and hydrogen-nitrogen self-ignition process largely depends on the tube length and initial pressure. For pure hydrogen experiments the tube diameter influence is difficult to specify as there is no explicit trend in the ignition limits for particular diameters. However, for 40 and 50 mm tubes, ignition limit for d = 10 mm is slightly lower than for other diameters. At the same time it should be taken into account that a larger number of experiments (156) was conducted for d = 10 mm than for d = 6 mm (96) or for d = 14 mm (108). The tube length dependence seems to be non-linear, especially for tubes shorter than 40 mm as there was no ignition for experiments for L = 25 mm and pressures up to around 16 MPa for any of the diameters considered [25,26]. Similar trend of rapid increase of ignition limit was reported by Grune et al. [16] for 30-40 mm tubes. It can be observed that addition of nitrogen considerably increases the P_{burst} necessary for the ignition to occur.

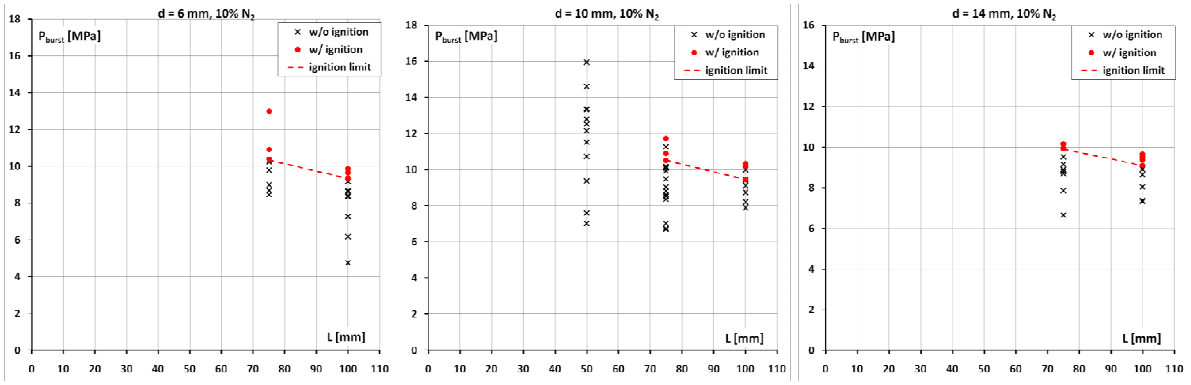

Figure 4. Cumulative diagrams of burst pressure ignition limit obtained for various extension channel lengths (10-100 mm) and diameters (6, 10, 14 mm) for cases with 10% N_2 addition to hydrogen

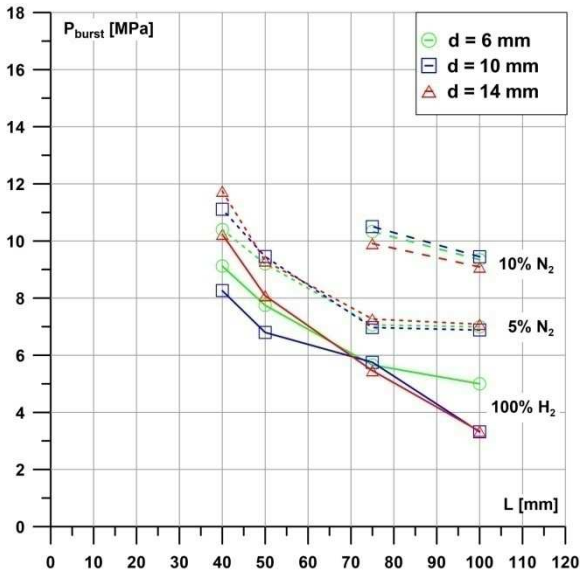

Figure 5. Comparison between burst pressure ignition limits obtained for pure hydrogen and hydrogen-nitrogen mixtures

Additionally, nitrogen addition seems to stabilise the self-ignition process independently on the tube diameter as ignition limit curves for 5% and 10% and respective diameters almost overlap. Slight discrepancies among specific diameters cases may be observed for 40 mm tube but a similar trend is visible for pure hydrogen and is probably caused by unstable ignition and combustion processes which result in the non-linear limit curve behaviour for shorter tubes. Table 1 presents the ratio between burst pressures obtained for H_2-N_2 mixtures ($P_{burst\ mix}$) and pure H_2 cases ($P_{burst\ H2}$) for corresponding geometries. The highest relative pressures ratios are present in the experiments with the longest tubes. Pressure ratios for d = 10 mm and d = 14 mm for corresponding tube lengths are in good agreement. However, d = 6 mm with L = 100 mm cases deviate from the rest of the ratios. It is caused by the fact that the ignition limit for d = 6 mm and L = 100 mm is higher (5.0 MPa) than for d = 10 mm (3.31 MPa) or d = 14 mm (3.33 MPa), thus it decreases the pressure ratio. This effect was observed by the authors during the experimental work and additional tests were done for d = 6 mm, L = 100 mm and burst pressures lower than 5 MPa to check if the ignition will occur. These tests however did not reveal any experiment with ignition.

Table 1. Experimentally obtained ignition pressures ratio $P_{burst\ mix}/P_{burst\ H2}$.

		5% N_2			10% N_2		
L	d	6 mm	10 mm	14 mm	6 mm	10 mm	14 mm
100 mm		1.4	2.08	2.12	1.87	2.85	2.72
75 mm		1.25	1.21	1.33	1.83	1.83	1.81
50 mm		1.19	1.39	1.15	-	-	-
40 mm		1.14	1.34	1.15	-	-	-

Based on the ideal shock tube assumptions [27], postshock temperature and pressure were calculated with the use of Cantera code [28]. The results of the calculations as a function of the initial pressure of the driver gas are presented in Fig. 6. For 100 mm tube, the temperature increase due to the change in driver gas mixture is observable only for d = 10 and 14 mm, for d = 6 mm temperature changes are only slight and oscillate around 1070 - 1085 K. As regards shorter tubes, 50 and 40 mm, the tendency is different, even though P_4 (P_{burst}) of the hydrogen-nitrogen mixture increases, the post-shock temperature decreases as much as 35–170 K in comparison to hydrogen cases for the same geometries. This comparison and scatter of results show that the ideal shock assumptions do not include some real effects present during the gas release including shock-shock, shock-wall interactions and the effect of the disk rupturing process. However, none of the postshock temperatures for experimentally obtained points is below the auto-ignition temperature of hydrogen-air at 1 atm (T = 858 K).

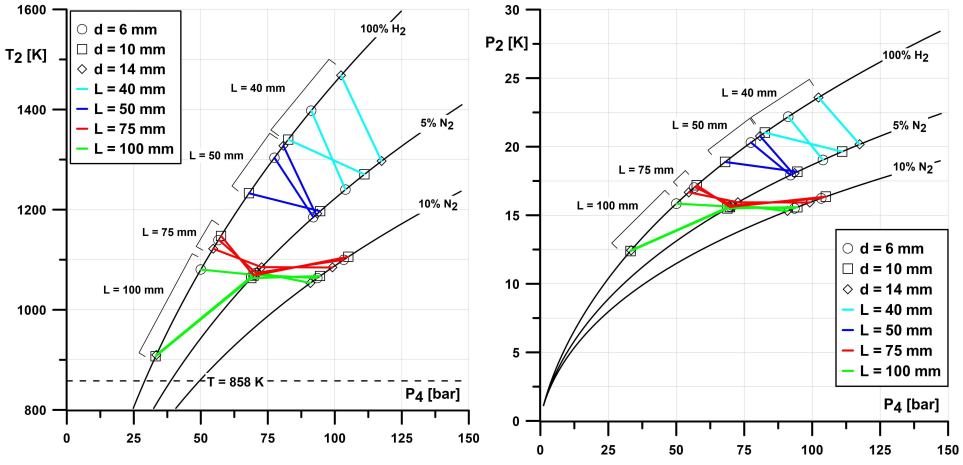

Figure 6. Postshock temperature (T_2) and pressure (P_2) as a function of driver gas initial pressure (P_4) and driver gas mixture. Points denote experimental results (ignition limit points from Fig. 5). Dotted line T = 858 K denotes hydrogen auto-ignition temperature in air.

3.0 NUMERICAL RESEARCH

3.1 Code description

The code utilized was based on KIVA3V code which is based on a Arbitrary-Lagrangian Eulerian (ALE) methodology [29]. It has been substantially modified by Wen and co-workers [19,21-24] specifically for modeling spontaneous ignition in pressurized hydrogen releases. ALE method is adopted to treat separately convective and diffusion terms considering the substantial scale difference between diffusion and advection. However, the demanding conditions of high-pressure gas release required modifications of the code including utilization of second-order Crank-Nicolson scheme for diffusion terms and the terms associated with pressure wave propagation, 3rd order TVD Runge-Kutta method for convection terms. For spatial differencing, the 5th order upwind WENO scheme [30] is implemented for the convection terms and the 2nd order central differencing scheme for all the other terms. Chemical reaction model was Saxena and Williams's [31] detailed chemistry scheme which involved 21 elementary reactions with 8 species. The scheme was previously validated against a wide range of pressures up to 3.3 MPa and used in previously referenced papers [19,21-24]. The scheme included third body reactions and reaction-rate pressure dependent "fall-off" behaviour. The chemical reaction kinetic equations are solved by a variable-coefficient ordinary differential equation (ODE) solver [32].

3.2 Geometrical model, initial and boundary conditions

The geometrical model selected for the calculations simulated an experimental stand geometry was composed of a part of the high pressure section and the extension tube of d = 10 mm and L = 50 mm. As it was stated during the experimental research, the self-ignition if occurred, took place in the extension tube, so farther geometry was not taken into consideration. Additionally, the geometry extension would significantly increase the calculation time. Experimental stand geometry was made of circular tubes so the numerical geometry was a 2-dimensional, axi-symmetrical domain (see Fig. 7). The mesh was structural with 15 x 15 µm cells in the extension tube, and orthogonal non-structural 15 ~ 150 µm in the high-pressure part of the domain. Total number of cells was slightly below 1200000.

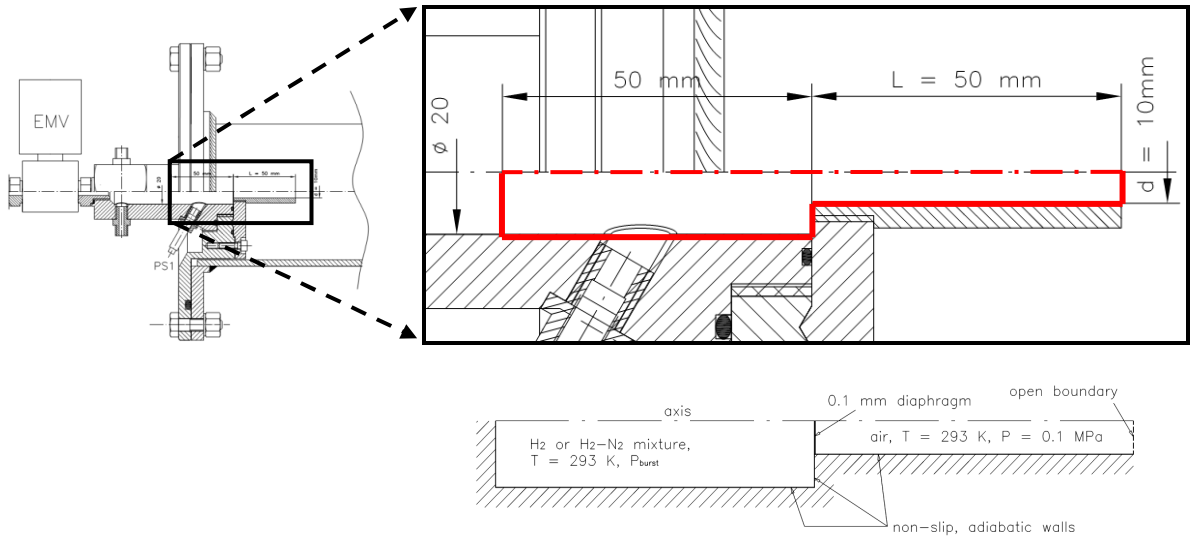

Figure 7. Geometrical model used in simulations (top) and boundary and initial conditions (bottom).

Simulations were performed for pure hydrogen and hydrogen-nitrogen mixtures with 5% and 10% of nitrogen addition. Initial temperature in the whole numerical domain was 293 K. Extension tube was filled with air being at 0.1 MPa, high-pressure part was filled with hydrogen or hydrogen-nitrogen mixture at variable pressures of 5 - 12 MPa. All cases considered are presented in table 2.

To simulate the diaphragm rupture process an Iris model [33] was used. Diaphragm with a thickness of 0.1 mm was mimicked by a cell-by-cell connection with linear rate of high-pressure and extension tube volume starting from the axis. The diaphragm opening time was defined as 5 μs based on the previously performed simulations [19].

Table 2. Numerical simulations performed with regards to burst pressure and driver gas composition

P_{burst} [MPa]	100% H_2	5% N_2	10% N_2
5	X		
6	X	X	
8	X	X	X
10	X	X	X
12			X

3.3 Results

The following figures illustrate the contours of density gradient and temperature (Fig. 8), OH and H_2 mass fractions (Fig. 9) for case with hydrogen being at initial pressure of 6 MPa. At the beginning of the simulation, density gradient shows the leading semi-spherical shock wave and following hydrogen gas. As the diaphragm opening rate is equal to 1000 m/s, at the time of fully opened diaphragm (5 μs) shock wave pattern consists of one leading semi-spherical and two oblique shock waves. The oblique shock waves reflect from the surrounding walls and interact with contact surface and leading shock. After few reflections they dissipate and transform to weak transverse shock waves. Due to the instabilities generated by shock waves and due to Rayleigh–Taylor instabilities, a toroidal vortex is produced. It is placed near the wall. As a result, hydrogen with shocked air mixing increases rapidly. The ignition spots are marked in Fig. 8 at simulation time of 16 μs. In all simulations with ignition, the reaction starts near the wall where air is double shocked, thus significant increase in temperature is generated. Further, the reaction zone development is supported by Kelvin-Helmholtz instabilities enhancing mixing near the wall where thin air layer is present. In Fig. 10 maximum temperatures during the simulations are presented for hydrogen initial pressures in the range of 6 - 10 MPa. For the time of 5 μs temperature peaks are observed for all of the simulations. As a result of fully opened diaphragm and for this time, oblique shock waves reached surrounding walls and increased the temperature locally. Depending on the initial pressure, after 1.6-3.2 μs later the following shock reflections occur and step by step increase the maximum temperature. However, the detailed OH mass fraction contours analysis showed that the ignition of a hydrogen-air mixture occurs around 10-16 μs of the simulation and starts near the wall (see circle marks in Fig. 9). For the 5 MPa case only one hot spot is observed on the wall. For the 6 MPa two hot spots appear and the second one is delayed to the first one with around 1 μs. As the reaction zones develop, they merge at around 25 μs of the simulation time and stay in the mixing layer near the wall up to the end of simulation. As regards the 8 MPa case two hot spots at one wall are generated: first one which is common for all cases, occurs at around 10 μs and extinguishes due to high hydrogen dilution in a toroidal vortex and the second one which shows up at around 15 μs and develops to steady reaction zone. Then a new strong ignition occurs in the place of the initially extinguished ignition spot at the vortex edge and finally, third hot spot shows up near the axis at around 19 μs and develops to the hydrogen-air contact surface. At the moment of hydrogen leaving the tube, two sustained reaction zones are present. In the 10 MPa simulation, first two ignition spots occur almost simultaneously at 10 μs and the third one in the axis at 13 μs. All of them develop into the steady reaction zone which propagates into the whole hydrogen-air contact surface. They merge together around 25 μs of simulation time. For the 5 and 6 MPa cases high temperature zones with reactions are present only in the vicinity of the wall. However, for the 8 and 10 MPa cases an additional reaction zone appears in the centre of the flow at hydrogen-air contact surface. This zone develops faster as the contact surface is more disturbed by stronger transverse

shock waves which enhance mixing. Thus, it is more probable for the flame to be sustained after leaving the tube for the cases with a developed reaction zone at the front contact surface than for reaction zone placed near the wall.

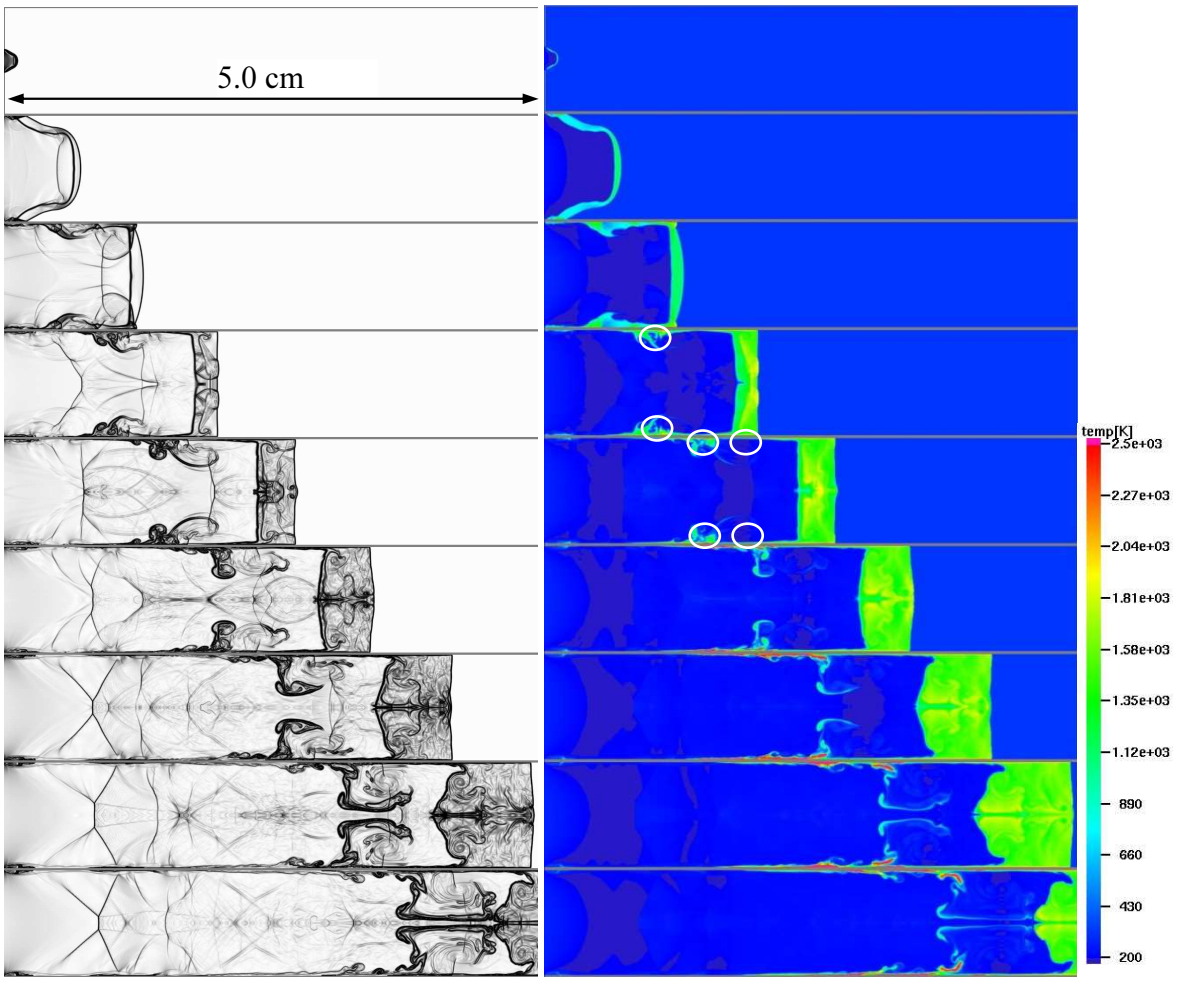

Figure 8. Density gradient and temperature contours for P_{burst} = 6 MPa; frames every 5 µs starting from 1 µs of simulation; white circles mark ignition spots at 16 µs further developed.

The ignition mechanism for mixture with 5% nitrogen addition is similar to observed for pure hydrogen cases, the ignition takes place in the vicinity of the wall where oblique shock waves reflect and interact with contact surface and leading shock. Similar as for pure hydrogen cases, the reaction zone development is supported by Kelvin-Helmholtz instabilities enhancing mixing near the wall where thin air layer is present. However, the ignition and following reaction zone development are shifted in burst pressure in comparison to pure hydrogen cases. For burst pressures 6 and 8 MPa only one ignition spot near the wall is present at around 17.5 and 16 µs respectively. For the 10 MPa case two ignition spots near the wall are generated at around 15 µs and third ignition spot in the axis shows up around 25 µs. As regards mixtures with 10% of nitrogen addition the flow pattern and ignition mechanism is similar to pure hydrogen and 5% nitrogen addition cases however additional increase in initial pressure is necessary to observe similar sequence as in previous simulations. In general, the simulations were distinguished according to the ignition spots number and the results obtained were compared with experimental results in Fig. 11. The comparison shows that the ignition with the following jet fire may be sustained only if three ignition spots are present and merge into the one reaction zone before leaving the tube which was recorded during the experiments as the photodiodes showed clear signal at the time of driver gas left the extension tube. The ignition criterion of merged ignition zones near the wall and in the axis was previously reported by Lee et al. [11,20] and experimentally confirmed by Kim et al. [13].

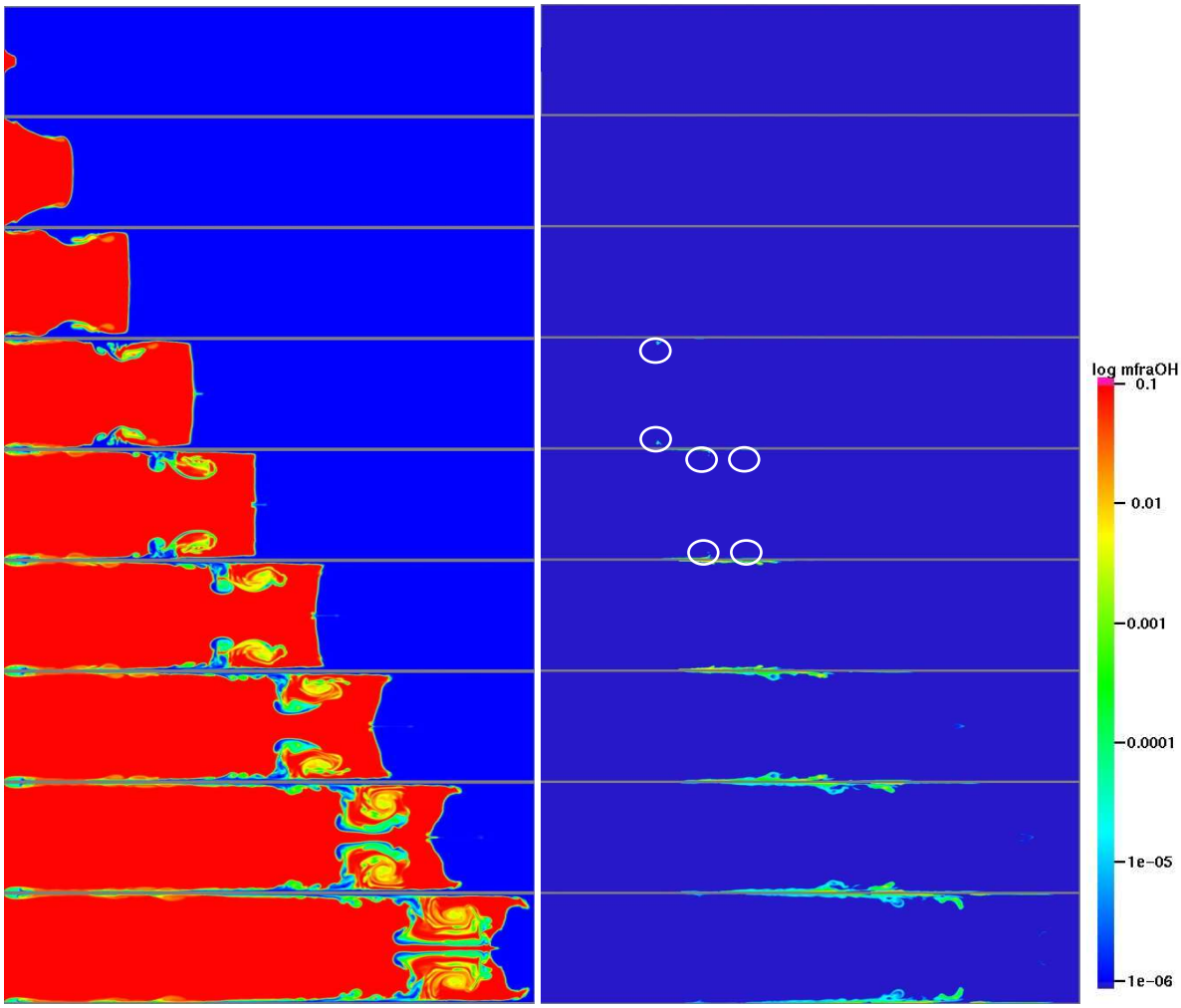

Figure 9. The H_2 and OH mass fraction contours for P_{burst} = 6 MPa; frames for every 5 µs starting from 1 µs of simulation; white circles mark ignition spots. The H_2 mass fraction in range of 0-1.

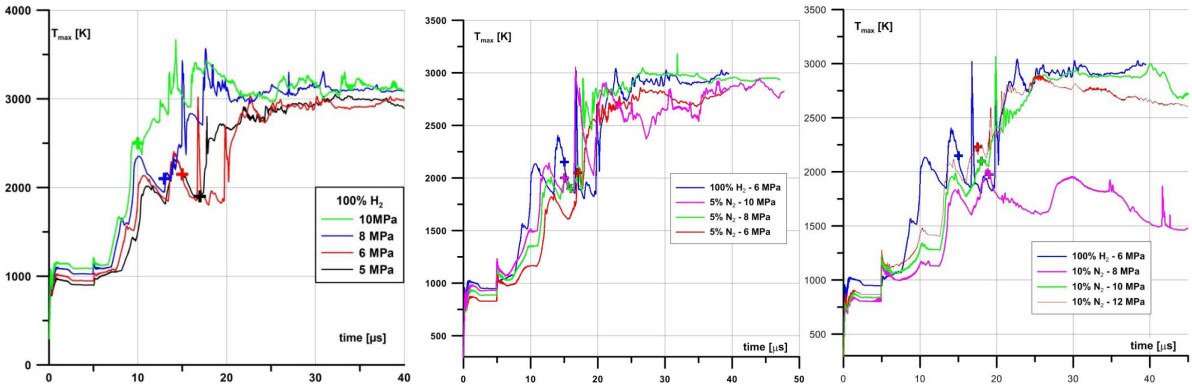

Figure 10. Maximum temperatures observed during the simulations for pure hydrogen (left), 5% nitrogen addition (centre) and 10% nitrogen addition (right) for various initial pressures. Crosses mark the approximated time where OH rich zones started to develop.

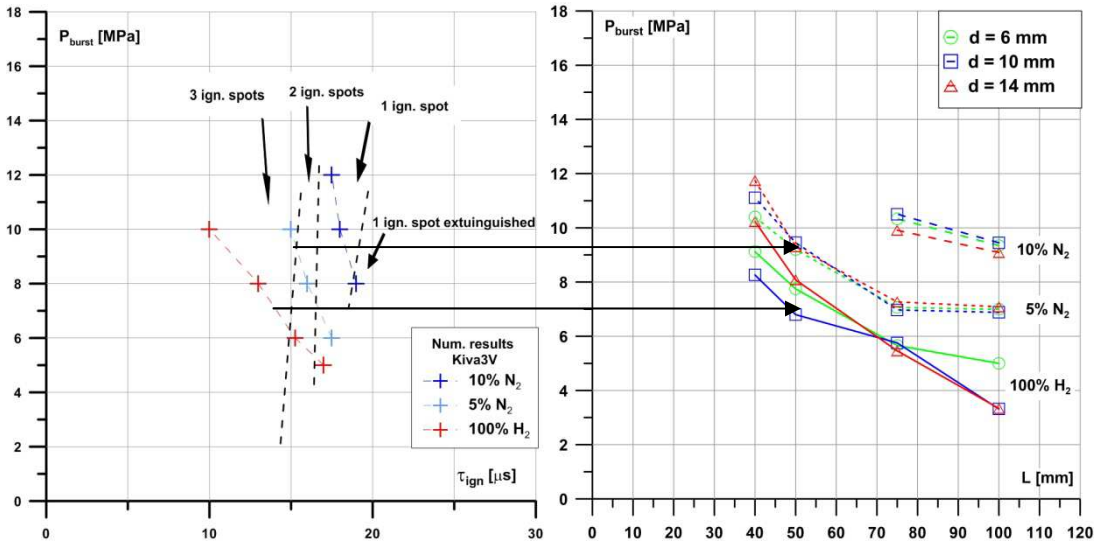

Figure 11. Numerically obtained ignition times according to the driver gas composition, burst pressure and ignition spot number (left) and experimentally obtained results as a function of tube length (right).

4.0 Summary and conclusions

In total, 295 experiments were conducted for hydrogen-nitrogen mixtures release: 213 for 5% N_2 and 82 for 10% N_2 addition. As a point of reference 360 previously performed experiments [25,26] with pure hydrogen release were used. Experiments showed that hydrogen and hydrogen-nitrogen mixtures self-ignition process largely depends on the tube length and initial pressure. Nitrogen doping considerably increases the mixture's initial pressure necessary for the self-ignition to occur. This effect is stronger for longer tubes and may increase the initial pressure as much as 2.12 or 2.85-times for 5% and 10% of nitrogen respectively in the mixture in comparison to the pure hydrogen case. Moreover, nitrogen addition seems to stabilise the self-ignition process independently on the tube diameter as ignition limit curves for 5% and 10% configuration almost overlap. Slight discrepancies among specific diameters cases for 5% N_2 addition may be observed for 40 mm tube but similar trend is visible for pure hydrogen and is probably caused by the unstable combustion for tube lengths close to the limiting (shorter) values. The Cantera ideal shock tube calculations showed that ideal shock assumptions do not include some real effects present during the gas release including shock-shock and shock-wall interactions. However, none of the postshock temperatures for experimentally obtained points is below the auto-ignition temperature of hydrogen-air (T = 858 K). Numerical simulations performed with modified KIVA3V code for hydrogen and hydrogen-nitrogen mixtures showed that the self-ignition process at the very beginning takes place in the vicinity of the wall where leading shock wave reflects. Depending on the burst pressure specific ignition sequence is present with one, two or three ignition spots. Third ignition spot is present at the tip region of the contact surface. Nitrogen addition to driver gas "shifts" the initial pressure necessary for the ignition sequence to occur. Comparison with experimentally obtained results showed that the criterion for sustained jet fire is that all of reacting regions should merge into the one reacting zone before the gas leaves the tube. This conclusion is consistent with previously referenced works [11,13,20].

ACKNOWLEDGEMENTS

This work has been financially supported by the European Union in the framework of European Social Fund through the "Didactic Development Program of the Faculty of Power and Aeronautical Engineering of the Warsaw University of Technology".

REFERENCES

1. NASA. Guidelines for hydrogen system design, materials selection, operations, storage, and transportation. Safety standard for hydrogen and hydrogen systems. Office of Safety and Mission Assurance, Washington, 1997, NSS 1740.16.
2. Anon, Spontaneous Ignition of Hydrogen, *Engineering,* **113**, 1922.
3. Wolanski, P., Wojcicki, S., Investigation into the mechanism of the diffusion ignitron of a combustible gas flowing into an oxidizing atmosphere, *Proceedings of the Combustion Institute,* **14**, 1972, pp. 1217-1223.
4. Mogi, T., Kim, D., Shiina, H. and Horiguchi, S., Self-ignition and explosion during discharge of high-pressure hydrogen, *Journal of Loss Prevention in the Process Industries* **21**, 2008, pp. 199-204.
5. Golub, V.V., Baklanov, D.I., Golovastov, S.V., Ivanov, M.F., Laskin, I.N., Savaliev, A.S., Semin, N.V. and Volodin V.V., Mechanisms of high-pressure hydrogen gas self-ignition in tubes, *Journal of Loss Prevention in the Process Industries* **21**, 2008, pp. 185-198.
6. Golub, V.V., Baklanov, D.I., Bazhenova, T.V., Golovastov, S.V., Ivanov, M.F., Laskin, I.N., Semin, N.V. and Volodin, V.V., Experimental and numerical investigation of hydrogen gas auto-ignition, *International Journal of Hydrogen Energy* **34**, 2009, pp. 5946-5953.
7. Oleszczak, P., Wolanski, P., Ignition during hydrogen release from high pressure into the atmosphere, *Shock Waves* **20**, 2010, pp. 539-550.
8. Dryer, F.L., Chaos, M., Zhao, Z., Stein, J.N., Alpert, J.Y., Homer, C.J., Spontaneous ignition of pressurized releases of hydrogen and natural gas into air, *Combustion Science and Technology* **179** (4), 2007, pp. 663-694.
9. Kim, S., Lee, H.J., Park, J.H. and Jeung, I.-S., Effects of a wall on the self-ignition patterns and flame propagation of high-pressure hydrogen release through a tube, *Proceedings of the Combustion Institute* **34** (2), 2013, pp. 2049-2056.
10. Mogi, T., Wada, Y., Ogata, Y. and Hayashi, A.K., Self-ignition and flame propagation of high-pressure hydrogen jet during sudden discharge from a pipe, *International Journal of Hydrogen Energy* **34**, 2009, pp. 5810-5816.
11. Lee, H.J., Kim, Y.R., Kim, S.-H. and Jeung, I.-S., Experimental investigation on the self-ignition of pressurized hydrogen released by the failure of a rupture disk through tubes, *Proceedings of the Combustion Institute* **33**, 2011, pp. 2351-2358.
12. Golub, V.V., Baklanov, D.I., Bazhenova, T.V., Bragin, M.V., Golovastov, S.V., Ivanov, M.F. and Volodin V.V., Shock-induced ignition of hydrogen gas during accidental or technical opening of high-pressure tanks, *Journal of Loss Prevention in the Process Industries* **20**, 2007, pp. 439-446.
13. Kim, Y.R., Lee, H.J., Kim, S.H. and Jeung, I.S., A flow visualization study on self-ignition of high pressure hydrogen gas released into a tube, *Proceedings of the Combustion Institute* **34**, 2013, pp. 2057-2064.
14. Kitabayashi, N., Wada, Y., Mogi, T., Saburi, T. and Hayashi, A.K., Experimental study on auto-ignition of high pressure hydrogen jets coming out of tubes of 0.1-4.2 m in length, International Conference of Hydrogen Safety – ICHS, San Francisco 12-14.09.2011, Paper no. 257.
15. Grune, J., Sempert, K., Kuznetsov, M. and Jordan, T., Experimental study of ignited unsteady hydrogen releases from a high pressure reservoir, *International Journal of Hydrogen Energy* **39** (11), 2013, pp. 6176-6183.
16. Grune, J., Sempert, K., Kuznetsov, M. and Breitung, W., Experimental study of ignited unsteady hydrogen jets into air, *International Journal of Hydrogen Energy* **36**, 2011, pp. 2497-2504.
17. Merilo, E.G., Groethe, M.A., Adamo, R.C., Schefer, R.W., Houf, W.G. and Dedrick, D.E., Self-ignition of hydrogen releases through electrostatic discharge induced by entrained particulates, *International Journal of Hydrogen Energy* **37**, 2012, pp. 17561-17570.
18. Bragin, M., Makarov, D. and Molkov, V., Pressure limit of hydrogen spontaneous ignition in a T-shaped channel, International Conference of Hydrogen Safety – ICHS, San Francisco 12-14.09.2011, Paper no. 171.

19. Wen, J.X., Xu, B.P. and Tam, V.H.Y., Numerical study on spontaneous ignition of pressurized hydrogen release through a lenght of tube, *Combustion and Flame* **156**, 2009, pp. 2173-2189.
20. Lee, B.J., Jeung, I.-S., Numerical study of spontaneous ignition of pressurized hydrogen released by the failure of a rupture disk in a tube, *International Journal of Hydrogen Energy* **34**, 2009, pp. 8763-8769.
21. Xu, B.P., Wen, J.X., Dembele, S., Tam, V.H.Y. and Hawksworth, S.J., The effect of pressure boundary rupture rate on spontaneous ignition of pressurized hydrogen release, *Journal of Loss Prevention in the Process Industries* **22**, 2009, pp. 279-287.
22. Xu, B.P., Hima, L.E., Wen, J.X., Dembele, S., Tam, V.H.Y. and Donchev T., Numerical study on the spontaneous ignition of pressurized hydrogen release through a tube into air, *Journal of Loss Prevention in the Process Industries* **21**, 2008, pp. 205-213.
23. Xu, B.P. and Wen, J.X., The effect of tube internal geometry on the propensity to spontaneous ignition in pressurized hydrogen release, International Conference of Hydrogen Safety – ICHS, 9-11.09.2013, Brussels, Belgium, Paper no. 201.
24. Xu, B.P., Wen, J.X., Tam, V.H.Y., The effect of an obstacle plate on the spontaneous ignition in pressurized hydrogen release: A numerical study, *International Journal of Hydrogen Energy* **36**, 2011, pp. 2637-2644.
25. Rudy, W., Dabkowski, A. and Teodorczyk, A., Experimental and Numerical Study on Spontaneous Ignition of Hydrogen and Hydrogen-Methane Jets In Air, *International Journal of Hydrogen Energy* **39**, 2014, pp. 20388-20395.
26. Rudy, W., The Influence of Gas Doping on Self-ignition of Hydrogen During High-pressure Release into Air, PhD thesis, Warsaw University of Technology, 2014.
27. Mark, H., The interaction of a reflected shock wave with the boundary layer in a shock tube, NACA, Technical Memorandum 1418, March 1958.
28. Goodwin D.G. Cantera user's guide. Pasadena, CA: California Institute of Technology; November, 2001.
29. Hirt, C.W., Amsden, A.A. and Cook, J.L., Arbitrary Lagrangian-Eulerian computing method for all flow speeds, *Journal of Computational Physics* **14**, 1974, pp. 227-253.
30. Jiang, G.S. and Shu, C.W., Efficient implementation of weighted ENO schemes, *Journal of Computational Physics* **126**, 2006, pp. 202-228.
31. Saxena, P. and Williams, F.A., Testing a small detailed chemical-kinetic mechanism for the combustion of hydrogen and carbon monoxide, *Combustion and Flame* **145**, 2006, pp. 316-323.
32. Brown, P.N., Byrne, G.D. and Hindmarsh, A.C., VODE, a Variable-Coefficient ODE Solver, *SIAM Journal of Scientific and Statistical Computing* **10**, 1989, pp. 1038-1051.
33. Goozee, R.J., Jacobs, P.A. and Buttsworth, D.R., Simulation of complete reflected shock tunel showing vortex mechanism for flow contamination, *Shock Waves* **15**(3), 2006, pp. 165-176.